

Monitoring and assessment of the structural effects due to ASR in Santa Luzia dam (Portugal)

José Piteira Gomes ⁽¹⁾, João Gomes Cunha ⁽²⁾, António Lopes Batista ⁽³⁾,
Fernando Almeida ⁽⁴⁾

- (1) National Laboratory for Civil Engineering (LNEC), Lisbon, Portugal, pgomes@lnec.pt
(2) EDP Gestão da Produção de Energia S.A., Porto, Portugal, joaogomes.cunha@edp.com
(3) National Laboratory for Civil Engineering (LNEC), Lisbon, Portugal, a.l.batista@lnec.pt
(4) EDP Gestão da Produção de Energia S.A., Porto, Portugal, fernando.almeida@edp.com

Abstract

The Santa Luzia dam, operated by EDP - Energias de Portugal, consists of two concrete arch structures. The main structure, located in a narrow gorge, is a thin arch with 76 m maximum height and a variable thickness in elevation, with a minimum of 2.5 m at the crest and 13.0 m at the bottom, while the secondary structure consists of a 27 m high arch-gravity to close a left bank cavity at high elevation. A V shaped buttress extends the main structure, functioning as an abutment. The dam was built between 1939 and April 1943. The narrow gorge was naturally formed by weathering and tectonic activity, in a quartzite outcrop. Quartzite aggregates were used in the dam's concrete mix.

The first signs of the swelling phenomena were identified in 1966, from the results of several geodetic surveys, due to the existence of progressive displacements at the crest, vertical upwards and radial upstream. Linear cracking at the downstream surface, parallel to the foundation, was also detected some years later. Physical and chemical tests were performed in the 1990s on samples taken from the dam body, to characterize the phenomenon itself and the changes that occurred in structural properties. Structural modelling has been used to interpret the observed behavior.

The paper presents some relevant monitoring results and its treatment, due in the scope of the dam's safety control activities, in order to allow an updated knowledge about the phenomenon itself and its structural effects.

Keywords: Santa Luzia dam; alkali-silica reaction (ASR); monitoring; structural assessment.

1. INTRODUCTION

Santa Luzia dam was the first arch dam built in Portugal, between 1939 and 1943. It is part of a pioneer hydroelectric scheme, at a time when Portugal increased the development of its hydroelectric capabilities. It was also the first dam studied by model tests at LNEC, some years after its construction.

A significant part of the mountainous region of the centre of Portugal is inserted, geologically, in the schist-greywacke complex of Beiras, which is crossed by a lot of quartzite outcrops. Santa Luzia dam was built on one of these outcrops. As they were available easily, quartzite aggregates, with very good mechanical properties, were used in the concrete composition. Alto Ceira and Pracana dams are also located on this geologic area and they were built with quartzite aggregate concrete too. These three dams were in Portugal, of the oldest, the most affected by expansive reactions of concrete. Pracana dam had a large rehabilitation in the decade of 1980 and Alto Ceira dam was replaced to a new one in 2013. The swelling magnitude in Santa Luzia dam has been smaller, which has allowed to manage the deterioration process with an adequate monitoring of behavior, carrying out some tests and studies and with small interventions in the dam, some of them related with improvements of the monitoring system. The main tests performed will be referred forward. Studies carried out in a timely manner have confirmed the satisfactory condition of the dam's serviceability and safety [1,2], so it has been operated with minor limitations.

The paper presents the relevant monitoring results, in terms of displacements, and its treatment, due in the scope of the dam's safety control activities, in order to allow an updated knowledge about the swelling process and its structural effects.

2. SANTA LUZIA DAM'S CHARACTERISTICS

2.1 Brief description of the dam

Santa Luzia dam is located on river Unhais, a tributary of river Zêzere. The dam was designed by André Coyne in the 1930s and was built between 1939 and April 1943.

The dam consists of two concrete arch structures. The main structure is a thin arch, with 76 m maximum height and a variable thickness in elevation with a minimum of 2.5 m at the crest and 13.0 m at the bottom, while the secondary structure consists of a 27 m high arch-gravity to close a left bank cavity at high elevation. A V shaped buttress extends the main structure, functioning as an abutment (Figure 2.1).

The rock mass foundation is heterogeneous and mainly consists of quartzites, except at the bottom of the valley and at the upper zone of the left bank, where quartzitic conglomerates occurred.

The available data about the composition and properties of the concrete are very reduced. In the concrete composition aggregates of a quartzitic nature were used, which were obtained by crushing at the dam site. The Portland cement mean contents was about 240 Kg/m³.

The first filling of the reservoir began on October 1942, before the dam was completed.



Figure 2.1: Santa Luzia dam. General view and cross section of the central cantilever

2.2 Swelling detection and following

In 1966, after some geodetic observation campaigns and site inspections, it was confirmed the existence of progressive swelling at the crest of the dam [3]. In 1991, a site inspection to the downstream and upstream faces, as well as a cracking survey were performed, which showed the existence of sub-horizontal cracks at mid-height of the main arch, parallel to the insertion surface, close to the foundation [4].

In 1995, three vertical cores, from the crest of the main arch, with 47 m depth, and a core in the arch-gravity, with 17 m depth, were drilled. These cores were intended to carry out different studies of analysis about the concrete weathering, including mineralogical and petrographic analyses. The main purpose was to identify the nature of the swelling products and try to quantify the swelling occurred, as well as the remaining potential reactivity. This study allowed the identification of products resulting from alkali-silica reactions, as well as the presence of swelling products of the ettringite and taumasite types, resulting from internal sulphate reactions. It was observed the presence of aggregates likely to provide alkalis to the reactions, which were released by the alteration of feldspars and micas. The analysis done to the cement paste led to conclude that a low alkali content cement was used in the concrete mix. The swelling tests, performed at a 35°C constant temperature, on specimens soaked in sodium hydroxide and potassium hydroxide solutions, showed, for a concrete about 50 years old, low residual swelling, of about 100×10^{-6} . Physical tests were also performed to characterize the concrete structural properties [5].

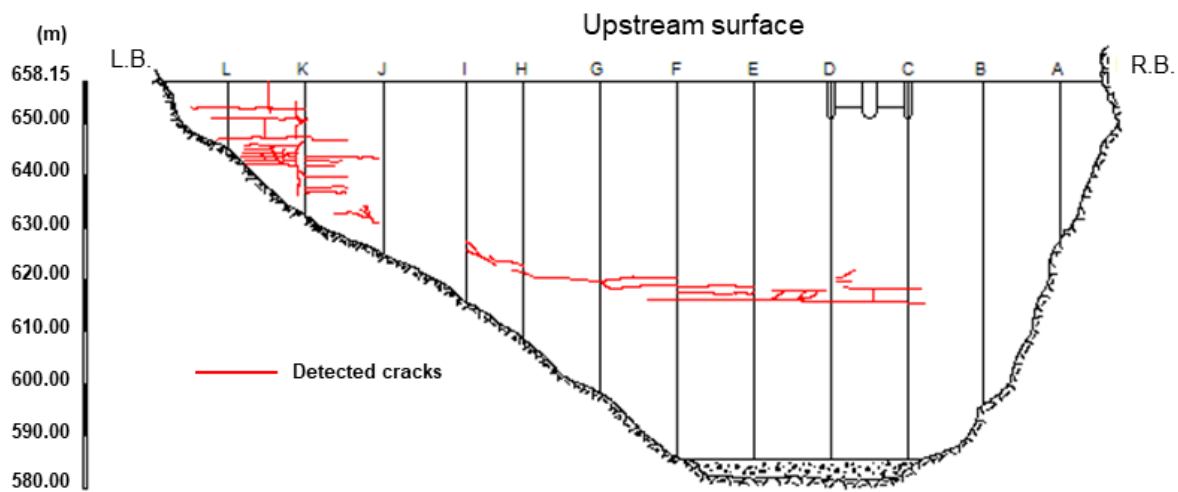


Figure 2.2: Results of crack survey of upstream surface due in November 1979

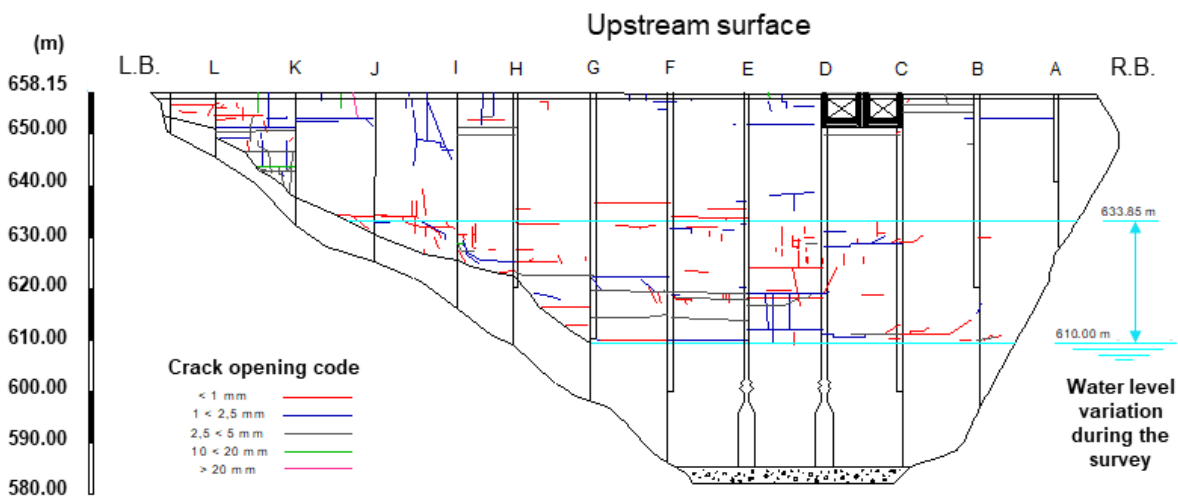


Figure 2.3: Results of crack survey of upstream surface due in October 1998

2.3 Monitoring system

The monitoring system has undergone several improvements over the years, because this was the first large concrete arch dam built in Portugal, where the first steps in dam's monitoring took place and it was necessary to introduce technological innovations that meanwhile appeared.

The initial monitoring system made possible to measure the following quantities: i) horizontal displacements at 9 points of the downstream surface of the main arch, using geodesic methods; ii) vertical displacement at 6 points of crest, by precision levelling; iii) strains in points of the downstream surface, with vibrating rope strain gauges; and iv) temperatures in the dam's body, with resistance thermometers.

In 1945, four more triangulation marks were placed on the downstream surface of the main arch and the position of an existing mark on the FG block was changed, having been defined the triangulation network that remains today (Figure 2.2).

The analysis of the results related to the measurement of strains and temperatures, carried out in 1948, showed that this equipment become nonoperational in 1946 and, consequently, was abandoned [3].

In September 1959, during the reservoir drawdown to the elevation 617,0 m, 12 jointmeters were installed to measure relative movements between blocks at the dam's contraction joints, 3 in the main arch and the remaining 9 in the arch-gravity structure. At this time, a drainage network was drilled in the gallery existing in the arch-gravity near the foundation, which allowed the control of drained flows and the uplifts measurement in some holes.

In 1987, eleven rod extensometers were placed to measure displacements of the foundation, 7 at the insertion of the main structure, 2 at the foundation of the shaped buttress (V) and 2 at the insertion of the arch-gravity, and three vertical rod extensometers, which cross the body of the dam in height, from crest to foundation. The monitoring system to measure the relative movements of joints and cracks, was reformulated either for having passed the measurement range of the instruments on existing bases or for need of control the relative movements on all joints of the main arch and several cracks, there were a total of 32 multiposition gages [6].

In 1995, a new reformulation of the monitoring system was implemented, having been installed an inverted plumb line anchored in foundation combined with a direct plumb line with a fixed end at crest of block DE, and an optical plumb line in the block BC, with access through a passageway at elevation 621,75 m, which allowed the measurements of the horizontal displacement independent of the geodetic monitoring system. Taking advantage of the holes drilled for the extraction of concrete samples, there were also installed 14 thermometers to characterize the temperature inside the concrete, 12 in the main arch and 2 in the arch-gravity. The system to monitoring the relative movements of joints and cracks was again reformulated by replacing multiposition gages that have passed the measurement range of the instruments and new 3D gages were installed to measure the movements of cracks that appeared at the elevation 616 m. Since then there are a total of 48 rosettes [6].

Figure 2.4 shows the current monitoring system for measuring horizontal displacements (plumb lines and geodesy) and vertical displacements at the crest (levelling line and R13 rod extensometer).

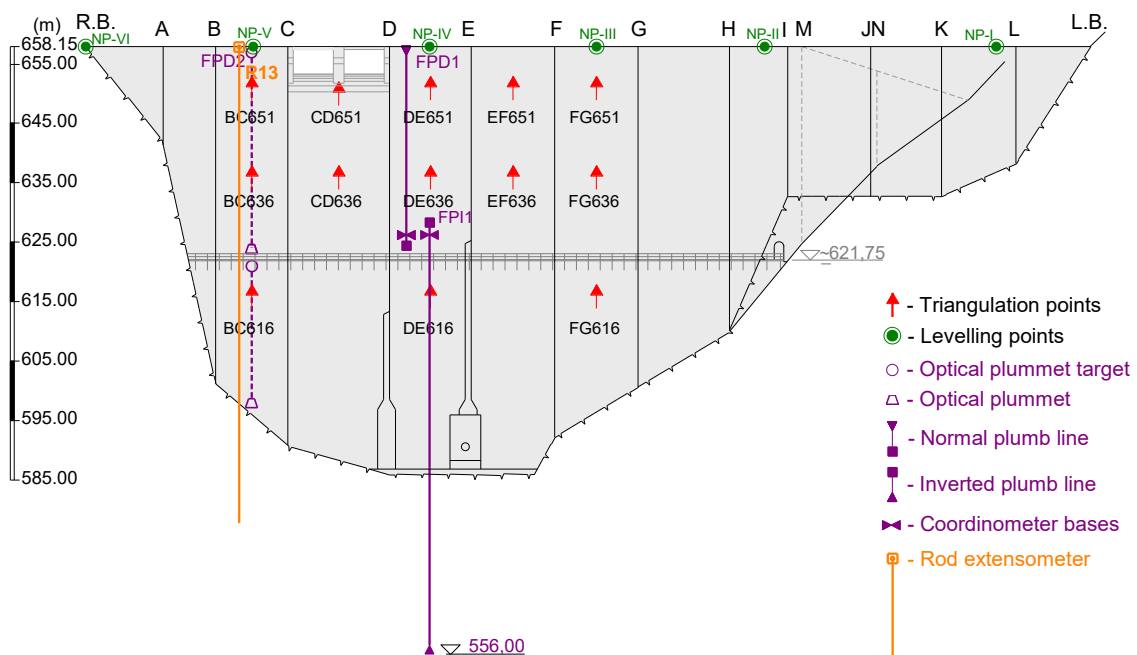


Figure 2.4: Monitoring instruments to measure horizontal displacements in the main arch and vertical displacements at the dam's crest

3. ANALYSIS AND INTERPRETATION OF THE OBSERVED BEHAVIOR

3.1 Statistical model adopted

The analysis and interpretation of the observed dam's behavior was carried out using a statistical model of quantitative interpretation of the displacements measured over time by geodetic methods and the central plumb line. Quantitative interpretation consists of the analysis of a behavior mathematical model by which a functional relationship is established between the quantities or effects observed and the actions that originate them. The principle of effects superposition is assumed, considering that the actions corresponding to hydrostatic pressures and seasonal variations in temperature cause reversible effects and that the irreversible effects, due to non-elastic phenomena, depend only on time. In the statistical model, a function of the type,

$$E_{calc}(h, t', t) = \sum_{i=1}^N a_i h^i + b_1 \cos \frac{2\pi t'}{365} + b_2 \sin \frac{2\pi t'}{365} + \sum_{j=1}^M c_j t^j + d \left(1 - e^{-\frac{t^n}{\beta}} \right) + k \quad (1)$$

was adopted, where E_{calc} represents the calculated response, h is the hydrostatic action usually represented by the upstream water level (when important, the downstream level must also be considered), t' is the number of days since the beginning of the year and t is the number of days counted from the initial observation date. The parameters a_i , b_1 , b_2 , c_j , d and k are calculated by linear regression, performed by the least-squares method. N and M represent the degree of the polynomials used to represent the hydrostatic pressure and time effects, respectively, the terms in sine and cosine are intended to represent the effect of the annual thermal wave, it is considered a polynomial expression to reproduce the time effects and an exponential term is used to represent the effects of expansive action. The differences between the values observed in the prototype and the values calculated by the statistical model are the residuals r , defined by the expression,

$$r = E_{obs}(h, t', t) - E_{cal}(h, t', t) \quad (2)$$

The coefficient of determination R^2 of a quantitative interpretation, which assesses the significance of the regression, is expressed by the equation,

$$R^2 = 1 - \frac{\sum_{i=1}^n (E_{cal}(h, t', t) - E_{obs}(h, t', t))^2}{\sum_{i=1}^n (E_{obs}(h, t', t) - \bar{E}_{obs}(h, t', t))^2} \quad (3)$$

where n is the number of observations and $\bar{E}_{obs}(h, t', t)$ is the average of the observed values. Closer the value of R^2 is to 1, more the model adjusts to the observed values.

3.2 Structural behavior interpretation

The first filling of the reservoir began in October 1942 and since then the dam has been continuously in operation, with several significant drawdown of the water level in the reservoir, particularly in the period between 1942 and 1959. After this period significant drawdown of the water level, more spaced in time, happened in October 1978 (614.3 m), October 1992 (625.1 m), August 1998 (617.0 m), March 2005 (624.4 m) and October 2014 (622.2 m). In Figure 3.1 the water level in the reservoir is presented from the first filling of the reservoir until January 2020.

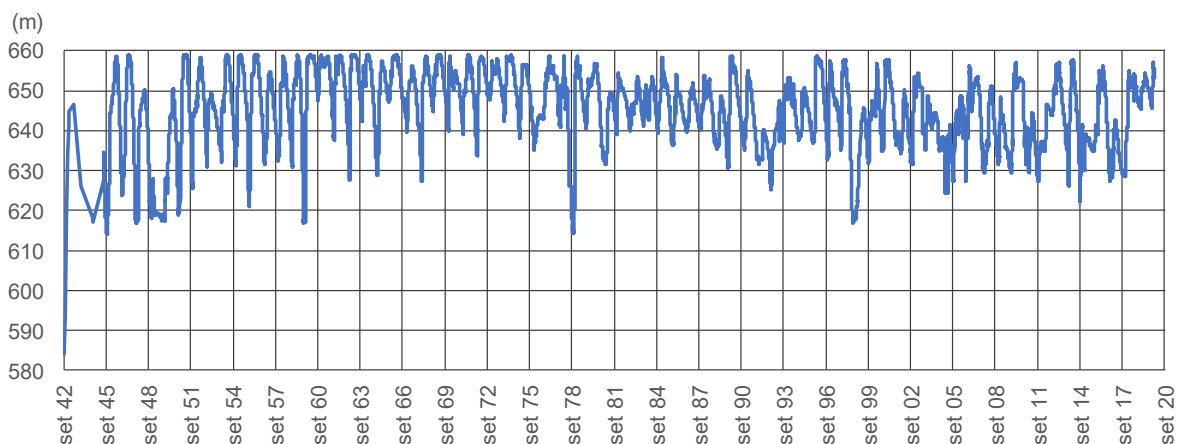


Figure 3.1: Water level in the reservoir since October 1942 until January 2020

Air temperature measurements started, through daily maximum and minimum records, only in January 2000. The recorded data allowed the computation of an annual period harmonic function as shown in Figure 3.2. The thermal air wave is characterized by the average value of 12.9 °C, an half-amplitude of 7.2 °C and a lag of 209.1 days related to the maximum annual value. In this period, the highest maximum and minimum lowest temperatures recorded were 34.9 C and -5.7 C, respectively.

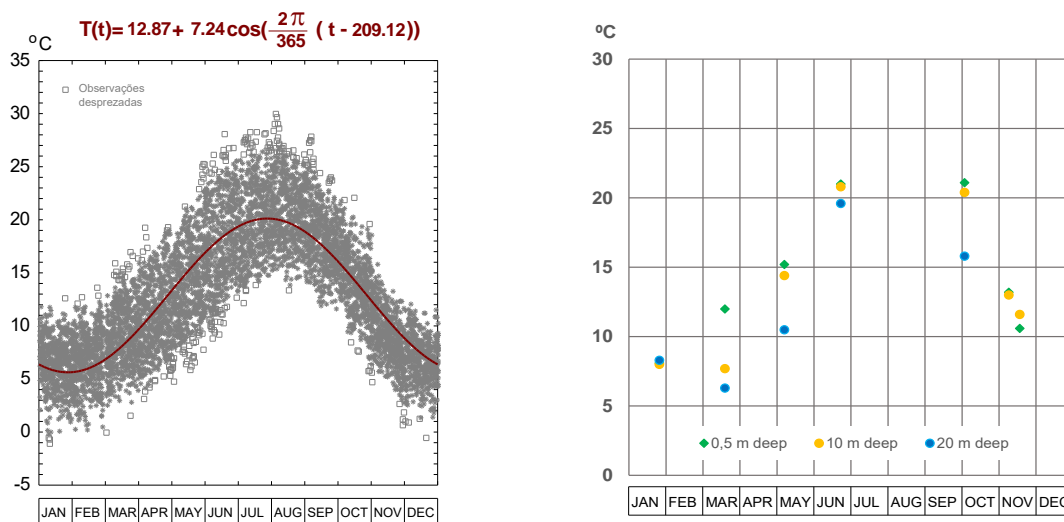


Figure 3.2: Daily maximum and minimum air temperatures observed and harmonic function adjusted (on the left), and reservoir water temperatures at depths of 0.5 m, 10.0 m and 20.0 m (on the right)

There are few data concerning the reservoir water temperature. The few records found refer to samples collected to carry out hydro-chemical analyzes of the reservoir water, beginning in March 2003, which are shown in Figure 3.2 for the depths of 0.5 m, 10.0 m and 20.0 m. It can be seen that the maximum and minimum temperatures are of 21.1 °C (October) and 6.3 °C (March), respectively.

Taking into account the dam age, in operation for nearly 80 years, it was decided to analyze its behavior considering three independent periods of similar duration, the first one between February 1943 and May 1970 (27 years), the second one between May 1970 and March 1996 (26 years) and the third one between March 1996 and November 2019 (23 years), in order to check possible differences in its structural behavior, assessed by the analyses of the horizontal and vertical displacements measured by different instruments. The 1996 date was chosen to take into account the installation of the plumb line in the block DE. It should be noted that the geodetic information available in each period is different, in the first period 14 campaigns were carried out, in the second period 16 and 23 in the third period, while 246 readings were collected on the plumb line throughout the period in which this instrument was operational.

3.3 Horizontal displacements analysis

For analysis of horizontal displacements, only some radial displacements are presented, the aforementioned statistical model was applied for those obtained by geodesic triangulation on point DE651 (block DE, elevation 651.0 m), in the three periods mentioned, as well as the displacements monitored on the plumb line, in the block DE at crest elevation (658.15 m), in the third period of analysis. A numerical model was used to evaluate the displacements in these two points of the block DE due to the hydrostatic pressure corresponding to the water level in the reservoir. This model, based on the finite element method [2], had considered an elastic-linear regime with the values of 20 GPa and 25 GPa to the concrete's elasticity modulus. In Figure 3.3 a) the elastic water level effect on the DE651 point is shown for the three time periods of geodetic data, as well as the same effect on the upper base of the plumb line at elevation 658.15 m, and also the results of the numerical model at elevation 651 m for the two values considered for the elasticity modulus. In Figure 3.3 b) the elastic water level effect on the upper coordinometer base of the plumb line installed on block DE at elevation 658.15 m, are presented, as well as the results of the numerical model at a central point of the block DE at elevation 658.1 m, for the two values considered for the elasticity modulus. It should be noted that the radial displacement at the crest is lower than the ones monitored and computed at elevation 651.0 m, which is due to the geometry of the dam.

From the quantitative interpretations carried out, based on geodetic data, the dam appears to have a different structural response to the water level action from the first to the second period, with significant loss of stiffness and an important deviation from the results obtained by the numerical model. The analysis of the geodetic data shows that there were no substantial changes in the response to the action of the water level variation between the second and third periods.

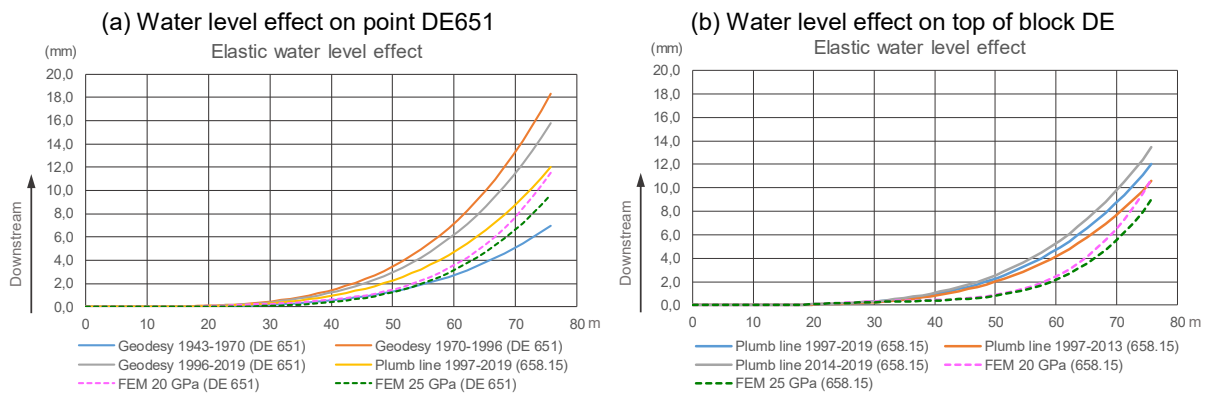


Figure 3.3: Elastic water level effects on points DE651, obtained from data collected on geodetic campaigns, and at crest (elevation 658.15 m) of block DE from readings on plumb line and FEM

The application of the statistical model to the collected data on the upper coordinometer base of the plumb line reveals a response to the water level variation compatible with the response given by the geodesic information on the DE651 point in the third period. However, like the results obtained by the geodesic method, the response of the structure presents an important deviation from the results obtained by the numerical model, what is admitted being due to loss of stiffness. Another relevant result of the application of the statistical model to the displacements measured on the plumb line, was the calculation of a function representing the time effects whose rate increases over time, when the history of the time effects in the radial displacements has consisted of a constant reduction in its rate. For this reason, this period from 1997 to 2019 was split in two, marked by the occurrence of a significant drawdown of the water level in December 2013 (626.7 m), according to that the first period was defined between October 1997 and December 2013 and the second one between January 2014 and December 2019. The purpose of this split was to search the drawdowns influence on the dam's response to hydrostatic pressure. As can be seen in Figure 3.3 b), there seems to have been a loss of structural stiffness associated with the referred drawdowns of the water level.

Regarding the thermal effect due to environmental actions, the results obtained by the statistical model also showed compatibility with the actions and an acceptable agreement between those obtained by the geodesic data and those resulting from the analysis of the data from the plumb line, namely the half-amplitude of the thermal wave function. In the case of the results obtained by the geodesic information in the first and second periods, a time lag is observed, that is due to the smaller number of campaigns carried out in these periods. In Figure 3.4 a) the thermal effect on the DE651 point is shown for the three periods of geodetic data, as well as the same effect on the upper base of the plumb line at elevation 658.15 m, are presented, and in Figure 3.4 b) the thermal effects on the upper coordinometer base of the plumb line installed on block DE at elevation 658.15 m are presented.

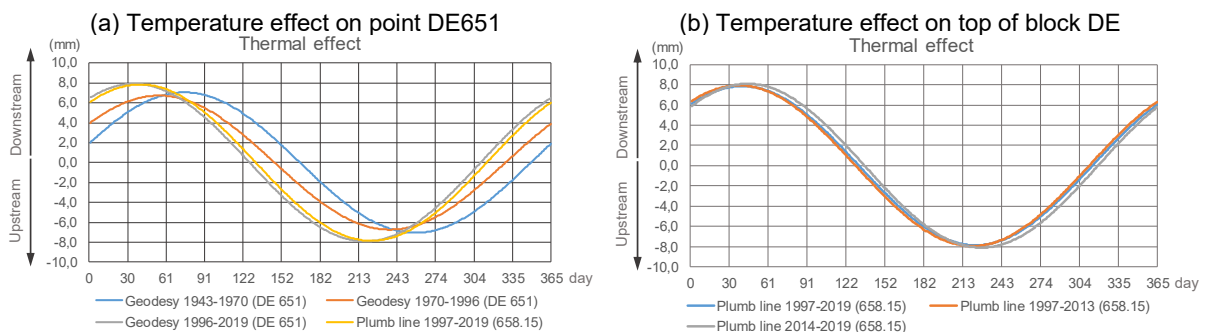


Figure 3.4: Temperature effects on points DE651, obtained from data collected on geodetic campaigns, and at crest (elevation 658.15 m) of block DE from readings on plumb line

Regarding the time effects, it should be noted that only in the first period (1943-1970) the concrete creep was considered, with the remaining time effects considered by a logarithmic function. In the remaining cases a second-degree polynomial function was used. Thus, based on geodetic data, irreversible displacements were obtained at point DE651 in the upstream direction, accountable to swelling, 19.5

mm at the end of the first period, 21.2 mm at the end of the second period and 11.4 mm in December 2013 in third period, as shown in Figures 3.5 a), 3.5 b) and 3.5 c), respectively. This last figure also shows the time effect functions obtained by the data from the coordinometer base at the 658.15 m elevation on the plumb line of the DE block. As can be seen on Figure 3.5 c), the results are compatible until December 2013, with the value of 9.9 mm. In the subsequent period, between January 2014 and December 2019, the statistical model presents a substantially different response on time effects. Figure 3.5 d) shows the radial displacements measured on the DE plumb line coordinometer base, at elevation 658.15 m, and the curve computed from the statistical model results. It is evident the difficulty of the model to reproduce upstream displacements in hot seasons, with water levels below elevation 640 m, and also to reproduce the drawdown of the water level effects, especially those that occur during the hot season.

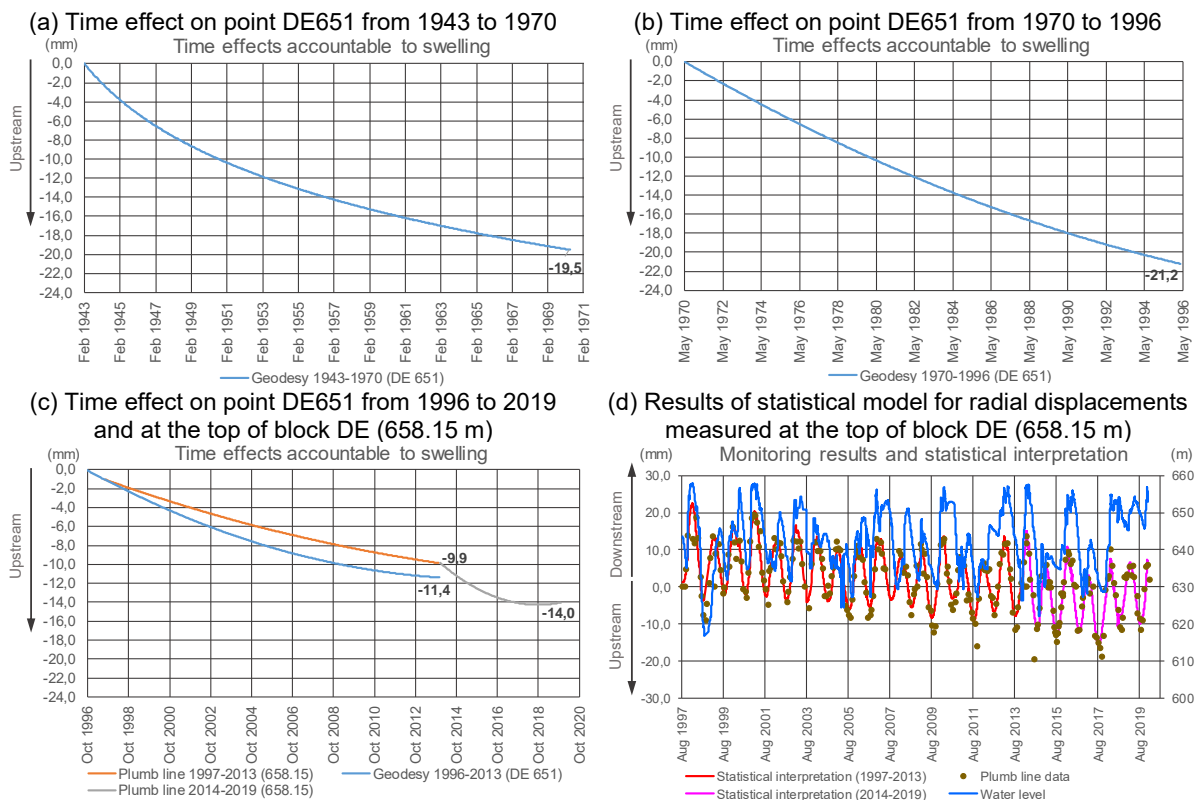


Figure 3.5: Time effects accountable to swelling on points DE651, obtained from data collected on geodetic surveys, and at the crest (elevation 658.15 m) of block DE from plumb line data

Also, the application of the statistical model to geodetic data shows the same difficulty in taking the radial displacements observed during the drawdowns of the water level, as can be seen in Figure 3.6, which integrates the results obtained in the three periods of analysis.

Finally, regarding the analysis of radial displacements, it should be noted that in the last three years a trend of irreversible displacements downstream has been observed, both through the analysis of geodetic data and the analysis from the plumb line data. The causes of these displacements drop are still under investigation.

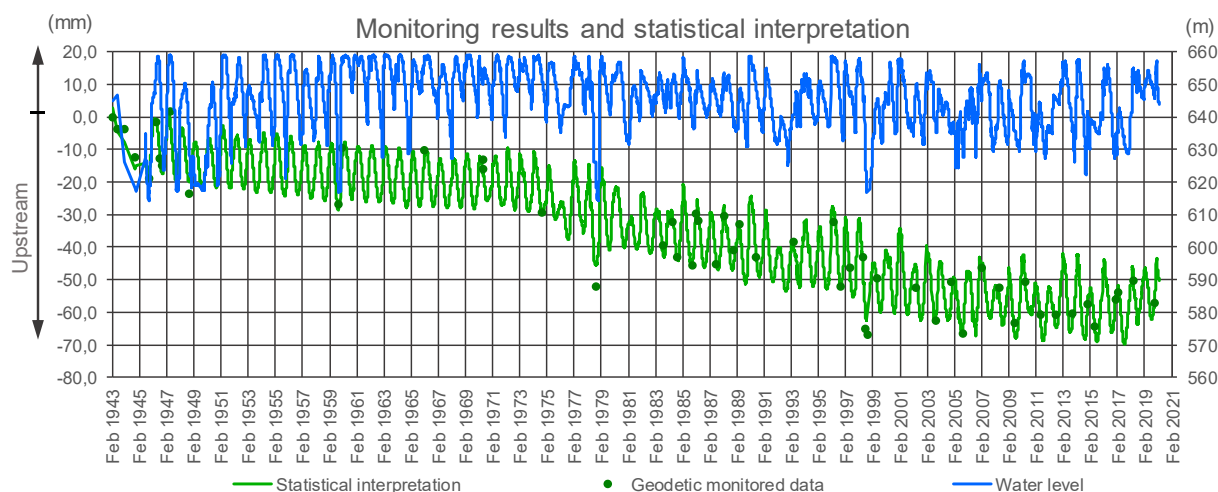


Figure 3.6: Results of statistical model application for radial displacements measured at point DE651 since February 1943 to November 2019

3.4 Vertical displacements analysis

The analysis of vertical displacements monitored by precision levelling was carried out with the aforementioned statistical model, at the six marks established in the initial leveling line configuration, on top of blocks KL, HN, FG, DE, BC and OA, whose reference campaign was performed on October 1945. It should be noted that the leveling line was reformulated in November 1988 with the installation of new marks on the top of the intermediate blocks.

Although the intention was to maintain the criterion of analyze the structural response to the same three periods separately, this was not possible because in the first period (1945-1970) only eight campaigns were carried out. Thus, it was analyzed the data collected on the second period, from May 1970 to March 1996 (16 campaigns), on the third period from May 1996 to November 2019 (36 campaigns), and also a longer period from October 1945 to March 1996 (24 campaigns) to cover the initial period. Thus, the displacements assigned to the first period were obtained by a simple difference between the displacements computed for the extended period and for the second period.

In Table 3.1 are presented the main results of the quantitative interpretation of vertical displacements, obtained from crest levelling for the second and third periods of analysis, being almost similar the results for the thermal effect in both periods, except in block DE, and a significant attenuation of the time effects, attributable to the expansive action, in the third period. There is also a greater sensitivity to the action of hydrostatic pressure in the third period.

Table 3.1: Main results of the statistical model applied to vertical displacements measured on levelling marks at the crest in the second and third periods of analysis

| Block | Mark | Vertical displacements (1970-1996) (mm) | | | Vertical displacements (1996-2019) (mm) | | |
|-------|------|--|---------------------|-------------------|--|---------------------|-------------------|
| | | Water effects | Temperature effects | Effects over time | Water effects | Temperature effects | Effects over time |
| KL | I | 0.6 | ±1.2 | 12.6 | -1.0 | ±1.3 | 8.7 |
| HN | II | -1.1 | ±2.9 | 22.8 | -3.3 | ±2.8 | 19.3 |
| FG | III | -0.6 | ±3.3 | 9.8 | -3.4 | ±3.0 | 6.2 |
| DE | IV | -1.8 | ±3.8 | 23.0 | -3.5 | ±2.9 | 12.0 |
| BC | V | -2.4 | ±2.9 | 10.9 | -3.4 | ±2.5 | 7.0 |
| OA | VI | -1.5 | ±1.2 | 1.3 | -1.6 | ±1.0 | 0.7 |

Vertical displacements upward are positive

Figure 3.7 shows the vertical displacements measured on mark IV, on top of block DE, at elevation 658.15 m, and the curve computed from the statistical model results. These results show a very significant reduction in the progression of vertical displacements towards the top of the dam's crest from

the second to the third period, being currently the swelling annual rate very small at mark IV of block DE.

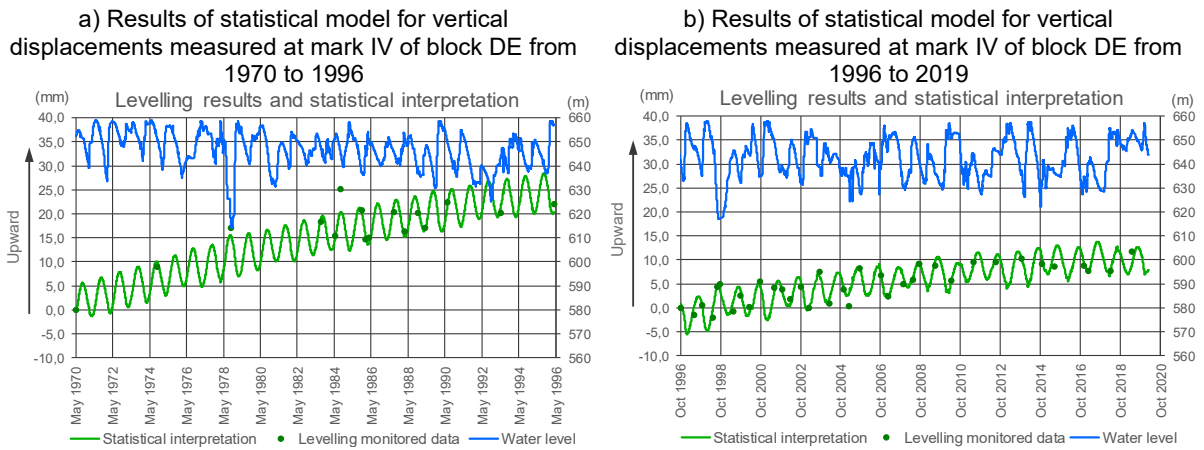


Figure 3.7: Results of statistical model application for vertical displacements measured at mark IV on top of block DE in the second and third periods of analysis

In Figure 3.8 the irreversible vertical displacements at the six marks at crest are presented, due to the swelling process, at the end of the second and third analysis periods. Although the elapsed time in the third period is less, it can be concluded that there was a significant attenuation of the swelling process, while not homogeneous. The results for the first period were calculated indirectly, as previously mentioned.

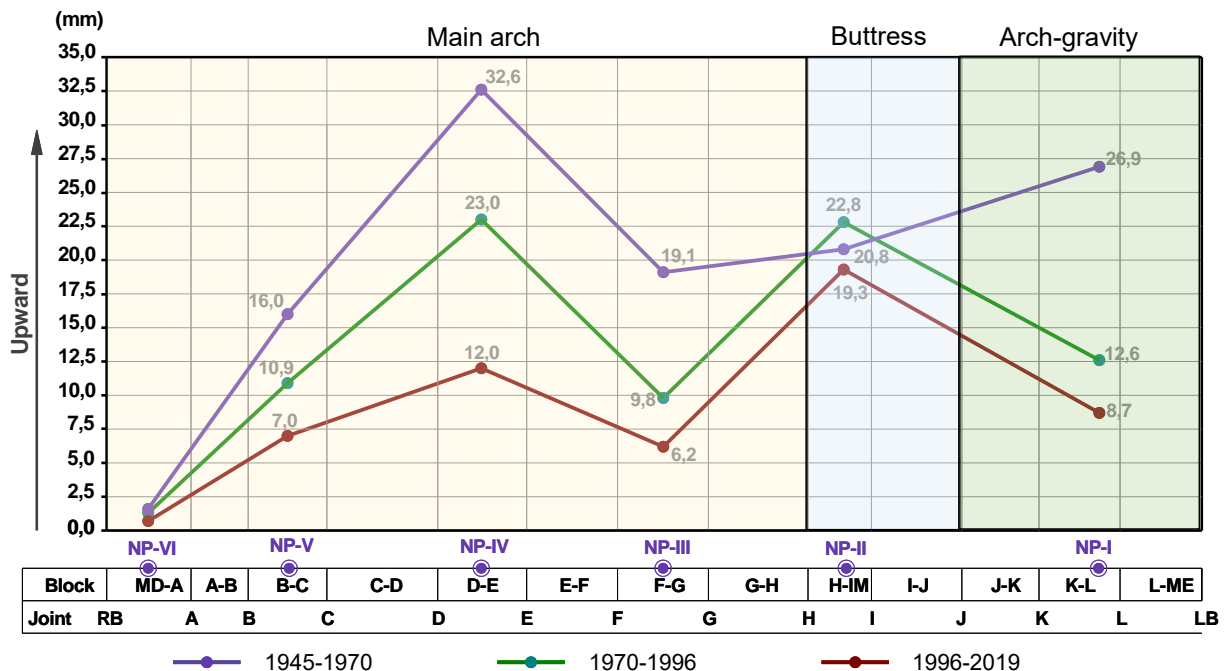


Figure 3.8: Irreversible vertical displacements computed for the levelling marks at the crest in the three periods of analysis

3.5 Swelling development

Based on the time effect components of the vertical displacements, computed by the quantitative interpretations from geodetic levelling data, the average values of the swelling developed in each block, for each one of the three periods of analysis, were evaluated. In Table 3.2 these results, at the end of

second and third periods, are presented, namely the accumulated irreversible displacements, the accumulated average strains and the average annual rates for all the points monitored.

In Table 3.3 the irreversible vertical displacements calculated for the extended period from October 1945 to March 1996 are presented and, by difference, the irreversible vertical displacements on the first period. The accumulated average strains and the average annual rates in the first period are also presented for the points monitored.

Table 3.2: Average swelling accumulated and average annual rates, computed from the time effects obtained at the end of second and third periods of analysis

| Block | Mark | Height (m) | 1970-1996 | | | 1996-2019 | | |
|-------|------|------------|---|---|---|---|---|---|
| | | | Accumulated vertical displacements (mm) | Accumulated vertical strains ($\times 10^{-6}$) | Annual swelling rate ($\times 10^{-6}$) | Accumulated vertical displacements (mm) | Accumulated vertical strains ($\times 10^{-6}$) | Annual swelling rate ($\times 10^{-6}$) |
| KL | I | 22.3 | 12.6 | 565 | 22 | 8.7 | 390 | 17 |
| HN | II | 51.3 | 22.8 | 444 | 17 | 19.3 | 376 | 16 |
| FG | III | 69.5 | 9.8 | 141 | 5 | 6.2 | 89 | 4 |
| DE | IV | 75.2 | 23.0 | 306 | 12 | 12.0 | 160 | 7 |
| BC | V | 69.0 | 10.9 | 158 | 6 | 7.0 | 101 | 4 |
| AO | VI | 6.0 | 1.3 | 217 | 8 | 0.7 | 117 | 5 |

Table 3.3: Average swelling accumulated and average annual rates, computed from the time effects obtained at the end of the extended period from 1945 to 1996 and calculated for the first period

| Block | Mark | Height (m) | 1945-1996 | | | 1945-1970 | | |
|-------|------|------------|---|---|---|---|---|---|
| | | | Accumulated vertical displacements (mm) | Accumulated vertical strains ($\times 10^{-6}$) | Annual swelling rate ($\times 10^{-6}$) | Accumulated vertical displacements (mm) | Accumulated vertical strains ($\times 10^{-6}$) | Annual swelling rate ($\times 10^{-6}$) |
| KL | I | 22.3 | 39.5 | 1771 | 35 | 26.9 | 1206 | 49 |
| HN | II | 51.3 | 43.6 | 850 | 17 | 20.8 | 405 | 17 |
| FG | III | 69.5 | 28.9 | 416 | 8 | 19.1 | 275 | 11 |
| DE | IV | 75.2 | 55.6 | 739 | 15 | 32.6 | 434 | 18 |
| BC | V | 69.0 | 26.9 | 390 | 8 | 16.0 | 232 | 9 |
| AO | VI | 6.0 | 2.9 | 483 | 10 | 1.6 | 267 | 11 |

As can be seen, it was during the first period (1945-1970) that the largest irreversible vertical strains occurred in the arch-gravity structure, 1206×10^{-6} at mark I on top of block KL, which have a strong attenuation in the second period to 565×10^{-6} , and a further reduction in the third period to 390×10^{-6} . These results are qualitatively in accordance with the appearance of intense horizontal cracking in this structural part. In the buttress, at mark II on the top of block HN, the strains computed in the three periods have similar values, being 405×10^{-6} , 444×10^{-6} and 376×10^{-6} in the first, second and third periods of analysis, respectively. In the main arch there were also reductions in vertical strains over time at the three points that have been observed since October 1945, mark III on top of block FG, mark IV on top of block DE, and mark V on top of block BC, being the highest value computed in block DE with 434×10^{-6} , 306×10^{-6} and 160×10^{-6} in the first, second and third periods of analysis, respectively.

Finally, in Table 3.4 the results obtained in the three periods are combined, to build a pattern of the current situation.

Table 3.4: Accumulated vertical displacements computed from October 1945 to November 2019 and respective average swelling and average annual rates

| Block | Mark | Height (m) | 1945-2019 | | |
|-------|------|------------|---|---|---|
| | | | Accumulated vertical displacements (mm) | Accumulated vertical strains ($\times 10^{-6}$) | Annual swelling rate ($\times 10^{-6}$) |
| KL | I | 22.3 | 48.2 | 2161 | 29 |
| HN | II | 51.3 | 62.9 | 1226 | 17 |
| FG | III | 69.5 | 35.1 | 505 | 7 |
| DE | IV | 75.2 | 67.6 | 899 | 12 |
| BC | V | 69.0 | 33.9 | 491 | 7 |
| AO | VI | 6.0 | 3.6 | 600 | 8 |

These results present a strong consistency with the apparent state of the dam, the observed deterioration is much more pronounced on the left bank blocks, that is, in the arch-gravity structure and in the buttress.

4. CONCLUSION

The displacements monitoring system of Santa Luzia dam was ruled, over a long period, from 1943 to 1997, only by geodetic methods, namely by horizontal displacements by triangulation on the main arch, since February 1943, and vertical displacements at crest by precision levelling, since October 1945. The foundation displacements measurements, by rod-extensometers, started in November 1987. In November 1988, the existing levelling line at crest was reformulated, with the introduction of new marks on the intermediate blocks. Finally, the monitoring of horizontal displacements by a plumb line placed in the block DE began in August 1997. The frequency of geodetic observation campaigns was not very regular, mainly in the first period between 1943 and 1970, in which 14 campaigns were carried out in 27 years but in the period between 1948 and 1959 there were no monitoring. It was from 1983 that geodetic campaigns began to be carried out with greater regularity, on an annual basis, although with some few years in which geodetic surveys were not performed.

The analysis carried out through the application of statistical methods to the displacements observed in three distinct and relatively long periods, with similar duration, allowed to get information about time periods with different structural behavior and also to have a global pattern of how the concrete deterioration process developed, due to internal swelling reactions. Intends to pave the way for a more refined analyses, namely adopting a numerical model that include the effects of chemical reactions, creep and the appearance and development of damage.

The analysis of the horizontal displacements only assesses the behavior of the main arch, showing that in the first period, from 1943 to 1970, there was greater stiffness of this structural part to the hydrostatic pressure action. It was in the second period, from 1970 to 1996, during which loss of stiffness occurred due to cracking. It was also possible to show that the response to the thermal action is very similar in the three periods of analysis. Regarding the irreversible displacements in the upstream direction, it was clear that its progression rate was higher in the second period, compatible with the loss of the structural stiffness, and also that in the third period there was a very significant attenuation of these displacements, configuring a possible exhaustion of the swelling reaction.

The analysis of the vertical displacements allows the assessment of the behavior of the three structural elements, the main arch, the arch-gravity and the buttress, which shows that there was a reduction in the irreversible vertical crest displacements upwards from the first to the second period and from the second to the third period, with exception of the buttress, where the values have been very similar. It also shows that in the first period, between 1943 and 1970, the time effects attributable to the swelling process had some expression in the main arch and in the buttress, with average annual rates between 9×10^{-6} and 18×10^{-6} , but a much more expressive development was recorded in the arch-gravity structure, with irreversible vertical strains greater than 1200×10^{-6} , at the block KL, and with an average annual rate four times higher than the average value developed in the other structural elements. These results corroborate with the appearance of horizontal cracks reported in several documents, the first one related with the visual inspection carried out during the drawdowns of the water level in September 1959

[4]. Finally, it is important to mention that the analysis of vertical displacements also reveals a significant reduction in progression rates in the third period, which is compatible with the swelling reactions exhaustion.

REFERENCES

- [1] Pinho Miranda M, Moura G, Paupério A (1987). Structural behavior model of Santa Luzia dam (in Portuguese). Conferência Ibero-Americana sobre Aproveitamentos Hidráulicos, LNEC, Lisboa.
- [2] Piteira Gomes J, Batista AL, Oliveira S (2004). Analysis of concrete dams under swelling processes. 12th International Conference on Alkali-aggregate Reaction in Concrete (ICAAR 2004), Beijing, 10p.
- [3] Hidrorumo (1994). Santa Luzia dam. Monitoring plan (in Portuguese). EDP, Porto.
- [4] LNEC (1960). Observation of Santa Luzia dam during the total reservoir empty in 1959 (in Portuguese). Report, LNEC, Lisboa.
- [5] LNEC (1991) – Visual inspection of Santa Luzia dam. Cracks and leakage (in Portuguese). Report, LNEC, Lisboa.
- [6] LNEC (1996) – Santa Luzia dam. Observation and analysis of concrete samples (in Portuguese). Report, LNEC, Lisboa.

Monitoring and assessment of the structural effects due to ASR in Santa Luzia dam (Portugal)
José Piteira Gomes; João Gomes Cunha; António Lopes Batista; Fernando Almeida